Journal of Geoscience and Environment Protection, 2023, 11, 60-85
https://www.scirp.org/journal/gep
ISSN Online: 2327-4344
ISSN Print: 2327-4336

Evaluation of Source Rock Potential for Hydrocarbon Generation in Shallow Offshore, Lamu Basin, Kenya

Dennis Ombati[1,2], Githiri John[1], Maurice K'Orowe[1]

[1]Department of Physics, Jomo Kenyatta University of Agriculture and Technology, Nairobi, Kenya
[2]Department of Physics, Kisii University, Kisii, Kenya
Email: dombatius@gmail.com

How to cite this paper: Ombati, D., John, G., & K'Orowe, M. (2023). Evaluation of Source Rock Potential for Hydrocarbon Generation in Shallow Offshore, Lamu Basin, Kenya. *Journal of Geoscience and Environment Protection, 11,* 60-85.
https://doi.org/10.4236/gep.2023.115004

Received: March 26, 2023
Accepted: May 21, 2023
Published: May 24, 2023

Abstract

The ever-increasing demand for oil and gas has driven its exploration in rather extreme conditions. In Lamu offshore, which is hitherto underexplored, most of the wells already drilled turned out dry save for a few wells with hydrocarbon shows despite the promising reservoir properties and related geological structures. This, therefore, necessitated a source rock evaluation study in the area to ascertain the presence and potential of the source rock by integrating the geochemical data analysis and petroleum system modeling. The shallow Lamu offshore source rock quantity, quality, and maturity have been estimated through the determination of the total organic carbon (TOC) average values, Kerogen typing, and Rock-Eval pyrolysis measurements respectively. Geochemical data for Kubwa-1, Mbawa-1, Pomboo-1, and Simba-1 were evaluated for determining the source rock potential for hydrocarbon generation. Petroleum system modeling was applied in evaluating geological conditions necessary for a successful charge within a software that integrated geochemical and petrophysical characterization of the sedimentary formations in conjunction with boundary conditions that include basal heat flow, sediment-water interface temperature, and Paleo-water depth. The average TOC of 0.89 wt % in the study area suggests a fair organic richness which seems higher in the late cretaceous (0.98 wt %) than in the Paleocene (0.81 wt %). Vitrinite reflectance and T_{max} values in the study area indicate the possible presence of both mature and immature source rocks. Type III Kerogen was the most dominant Kerogen type, and gas shows are the most frequent hydrocarbon encountered in the Lamu Basin with a few cases registering type II/III and type II. The charge properties (i.e. Temperature, transformation ratio, and Vitrinite reflectance) over geologic time at each of the wells have been estimated and their spatial variation mapped as seen from the burial history and depth curves overlaid with temperature, transformation ratio, and Vitrinite reflectance respectively. From the upper cretaceous maturity maps, the results seem to favor near coastal regions where average TOC is about 1.4 wt %, Vitrinite reflectance is more than 0.5%, transformation ratio is more than 10%, and temperatures range from 80˚C to 160˚C. The results postulate the absence of a definitive effective source rock with a likelihood of having cases of potential and possible source rocks. Moreover, greater uncertainty rests on the source rock's presence and viability tending toward the deep offshore. Geochemical analysis and petroleum system modeling for hydrocarbon source rock evaluation improved the understanding of the occurrence of the possible and potential source rocks and processes necessary for hydrocarbon generation.

Keywords

Geochemical Analysis, Petroleum System Modeling, Rock-Eval Pyrolysis, Kerogen Typing, Vitrinite Reflectance, and Transformation Ratio

1. Introduction

The ever-increasing demand for oil and gas has driven its exploration in rather extreme conditions. In Lamu offshore, which is hitherto underexplored, most of the wells already drilled turned out dry save for a few wells with hydrocarbon shows despite the promising reservoir properties and related geological structures. This, therefore, necessitated a source rock evaluation study in the area to ascertain the presence and potential of the source rock by integrating the geochemical data analysis and petroleum system modeling.

A source rock is rich in organic matter, which, if heated sufficiently, will generate oil or gas. Typical source rocks, usually shales or limestones, contain about 1% organic matter and at least 0.5% total organic carbon (TOC), although a rich source rock might have as much as 10% organic matter. The quantity of organic matter is commonly assessed by a measure of the total organic carbon (TOC) contained in a rock. Quality is measured by determining the types of Kerogen in the organic matter. Thermal maturity is most often estimated using Vitrinite reflectance measurements and data from pyrolysis analyses (Waples, 1994).

The Lamu Basin has potential source rocks ranging from type I to type III Kerogen (NOCK, 1995). These include Jurassic Oolitic Limestone and Lacustrine shales, with an average TOC of 1.4%. Type III Kerogen is the most dominant Kerogen type, and gas occurrences are the most frequent hydrocarbon encountered in the Lamu Basin (Ngechu, 2012). Jurassic to Cretaceous source rocks is widely distributed with good quality and is the primary source rocks on the east coast of Africa. Tertiary source rocks have a lower thermal evolution degree and are considered ineffective source rocks in all basins except Somali Basin (Nyaberi & Rop, 2014).

Lamu Basin has bad source rock conditions, with an inference of a possible presence of two sets of source rocks and a lack of high-quality source rock (Zhou et al., 2013). The Lamu basin source rock's nature and maturity remain crucial (Osicki et al., 2015). The charge, (primarily source presence), is the critical risk for deep offshore Lamu Basin, with no definitive evidence of deep-water marine source rock in the Basin. Since the source rock presence is unproven, great uncertainty in finding the source rock potential stratigraphic interval rests in deep offshore (Osukuku et al., 2022).

The purpose of this study is to evaluate the source rock's presence and potential using geochemical data analysis and applying petroleum system modeling in evaluating geological conditions necessary for a successful charge. Geochemical data for Kubwa-1, Mbawa-1, Pomboo-1, and Simba-1 were evaluated for determining the source rock potential for hydrocarbon generation. Petroleum system modeling was applied in evaluating geological conditions necessary for a successful charge within a software that integrated geochemical and petrophysical characterization of the sedimentary formations in conjunction with boundary conditions that include basal heat flow, sediment-water interface temperature, and Paleo-water depth.

2. Geological Setting and Study Area

The Lamu basin extends to an area of about 255,000 km^2 covering both the onshore and offshore whereby the thickness of the sediments ranges from 3 km to 10 km onshore and 12 km near the coastline to less than 3 km offshore, thinning towards the deep Indian ocean. The geology of Lamu Basin is tectonically controlled (Kimburi et al., 2015). These tectonic activities brought about the splitting of Gondwana during the Jurassic and the Anza Rift Cretaceous activity. The Lamu Basin belongs to a passive continental margin classification and is unusual in that it lies in a transitional position between a rifted margin to the North in Somalia and a transform margin to the south. Carbonates, shales, and marine sandstones constitute the sediments of the area (**Figure 1**) (NOCK, 1995).

South-Eastern Kenya's Lamu basin relates to the rifted continents like Australia, America, India, Antarctica, Africa, and Madagascar during the Jurassic rifting (Coffin & Rabinowitz, 1987). East Africa's potential for hydrocarbons is signified by the significant oil and gas discoveries in Mozambique and Tanzania and the heavy oil deposits in Madagascar's conjugate margin (Osicki et al., 2015). Following the worldwide scale for exploration status and success rate, computed according to the number of drilled exploration wells per 5000 km^2, the exploration status and success rate in Kenya remain very low. However, the prospective offshore Lamu basin of Kenya, (**Figure 2**), has received much interest in hydrocarbon exploration, the exploration potential defined by the ratio of success rate to exploration status stands fair (51%) compared to other basins in Kenya (Nyagah et al., 1996).

Despite the gas and oil shows evidenced by a few of the drilled twenty (20)

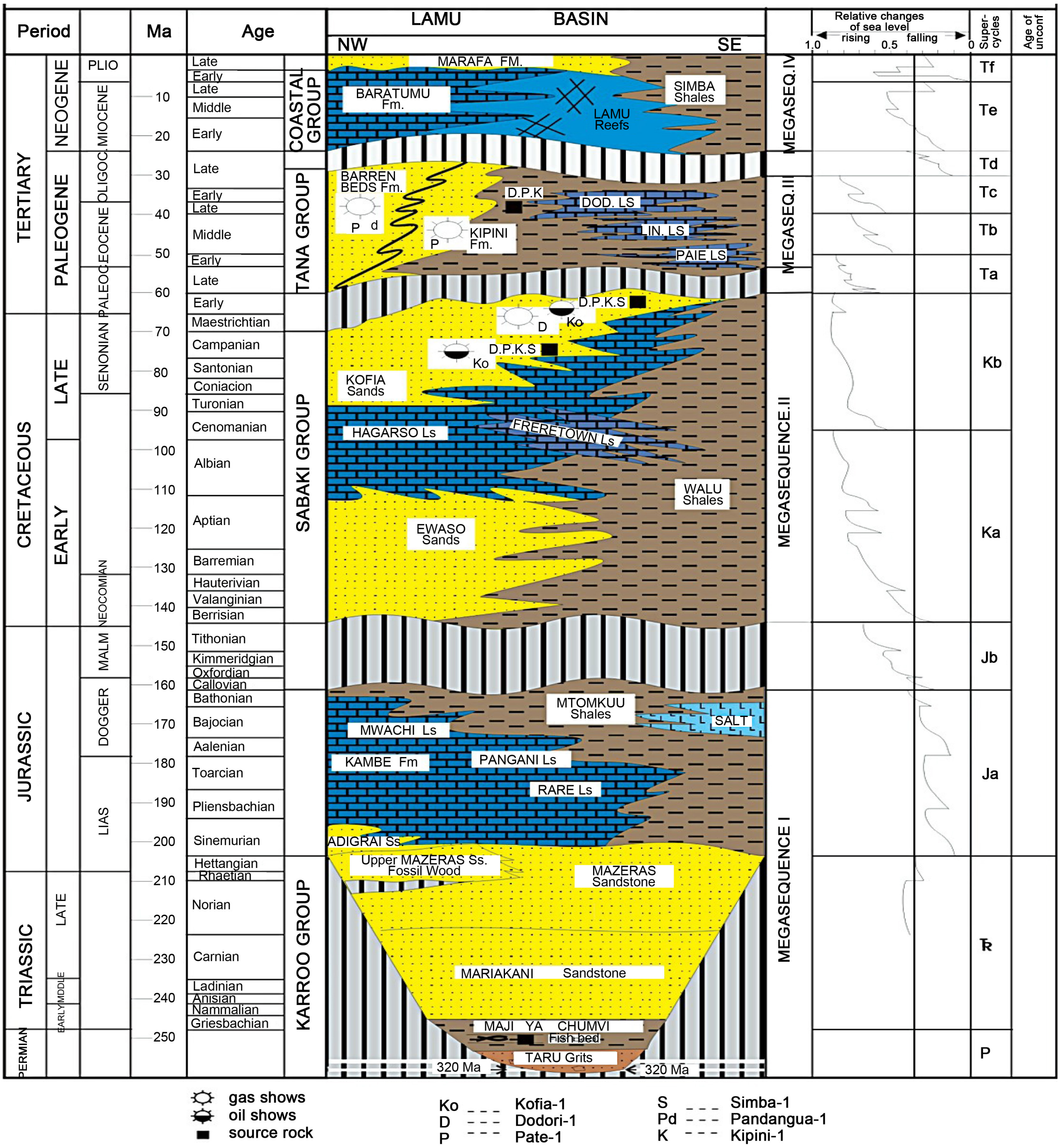

Figure 1. Chronostratigraphic chart showing Lamu basin events from Triassic through to Tertiary (Nyagah, 1995).

exploration wells, most of the drilled wells turned dry (**Figure 3**). The purpose of this paper, therefore, is to apply petroleum system modeling in evaluating geological conditions necessary for a successful charge. Petroleum Systems Modeling (PSM) is a vital component of exploration risk assessment and is applicable during all stages of exploration, from frontier basins with no well control to well-explored areas (Ruffo et al., 2006). Petroleum system models require geochemical and petrophysical characterization of the sedimentary formations in

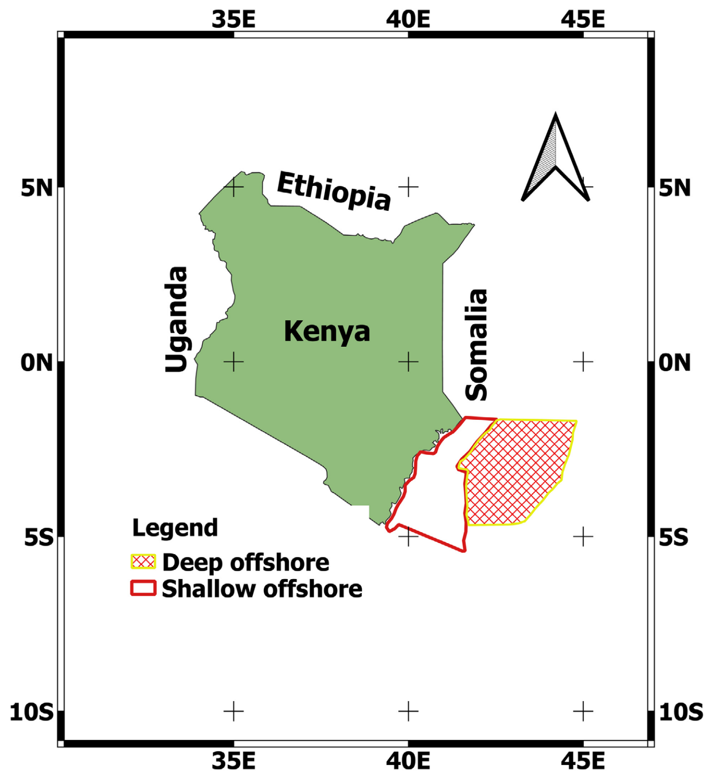

Figure 2. Map of Kenya showing the area of study outlined in red (Modified from NOCK Library).

conjunction with boundary conditions (paleo-water depth, sediment-water interface temperature, and basal heat flow) (Al-Hajeri et al., 2009).

3. Hydrocarbon Source Rocks Evaluation

Prediction of the presence of viable source rock is a vital prerequisite before exploration effort advancement in a new basin. Due to limited well control that could provide source rock interval direct evidence, the application of seismic geometries and petroleum system modeling are preferred in many cases (Liner & McGilvery, 2019). To be a source rock, a rock must have a quantity of organic matter, quality capable of yielding moveable hydrocarbons, and thermal maturity features (**Table 1**). The first two components are products of the depositional setting. The third is a function of the structural and tectonic history of the province. Various criteria exist in source rock classification (Al-Areeq, 2018). According to Waples (1994), source rocks can be distinguished into potential, possible, and effective whereby potential source rocks are the immature sedimentary rocks capable of generating and expelling hydrocarbons if their level of maturity were higher. Possible source rocks are sedimentary rocks whose source potential has not yet been evaluated, but which may have generated and expelled hydrocarbons, and effective source rocks are sedimentary rocks, which have already generated and expelled hydrocarbons. Source rocks can also be classified as immature, mature, and post-mature regarding their oil generation

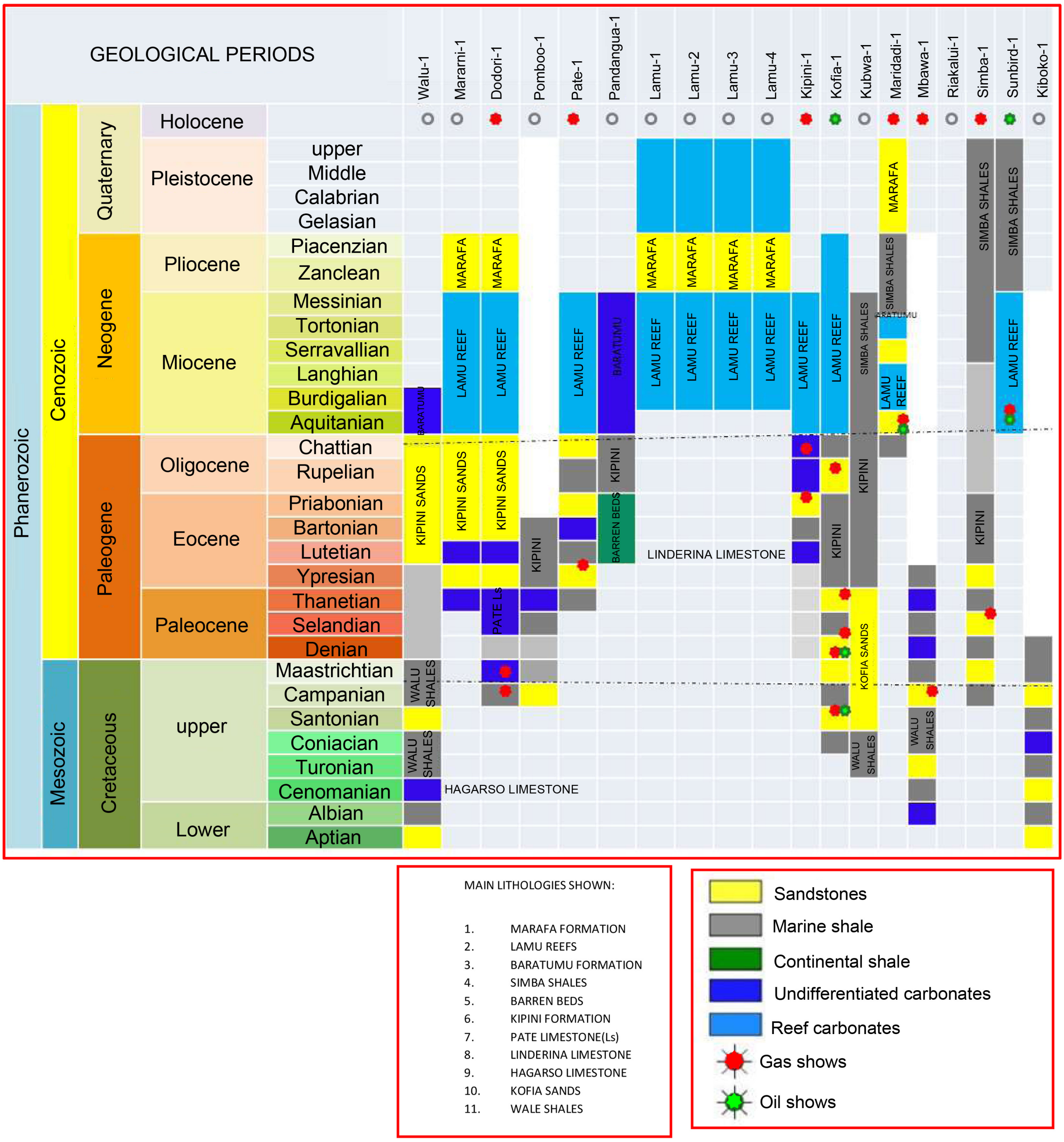

Figure 3. Wells stratigraphic information with highlighted main rift phases and identified main lithologies and formation names (modified from Beicip-Franlab).

(Hunt et al., 2002).

3.1. Using Geochemical DATA

The quantity of organic matter is commonly assessed by a measure of the total organic carbon (TOC) contained in a rock. Quality is measured by determining the types of Kerogen contained in the organic matter and the prevalence of

Table 1. Parameters for source rock evaluation (modified from JOGMEC).

maturity	R_o (%)	0.5		1.3		
		immature	Oil zone		Gas zone	
	T_{max} (˚C)	430		465		
		immature	Oil zone		Gas zone	
Kerogen Type	HI mg HC/g TOC	200		300		
		III (gas-prone)	II/III (oil/gas)		II (oil-prone)	
Organic richness	TOC (%)	0.5		1		
		Poor	Fair		Good	
		1		3		
		Poor	Fair		Good	

long-chain hydrocarbons. Thermal maturity is most often estimated by using Vitrinite reflectance measurements and data from pyrolysis analyses (Katz, 1983). TOC and Rock-Eval pyrolysis is the handiest method to evaluate organic richness, Kerogen type, and maturity. It is often used as a routine screening tool to find a good source interval (Peters & Cassa, 1994).

Rock-Eval is a standard routine analysis of source rocks, usually shales, to establish how much of the Kerogen has been transformed into petroleum and how much can be transformed at a higher temperature (Langford & Blanc-Valleron, 1990) (**Figure 4**). The sample of shale is crushed and heated to 300˚C, at which point one measure the amount of hydrocarbons that are already formed in the source rock but have not migrated out. The content of hydrocarbon with carbon numbers between C_1 and C_{25} is called S_1. It is measured as the area beneath the peak S_1. On further heating from 300 to 550˚C - 600˚C, new petroleum is formed in the laboratory from the Kerogen by heating (pyrolysis), and this amount is called S_2. This is a measure of how much oil and gas could have been generated if the source rock and been buried deeper. The reason it requires such high temperatures is that the heating in the laboratory lasts just a few minutes or hours, instead of some millions of years (Bjørlykke, 2010).

Figure 4 shows how a rock sample, representing a possible source rock, is heated gradually to about 550˚C while the amount of hydrocarbons generated is measured. At about 300˚C oil and gas which has already been generated in the source rock is expelled and measured as the S_1 peak. The peak at about 400˚C - 460˚C represents the amount of hydrocarbons generated from the Kerogen in the sample. The temperature of peak HC generation is called the T_{max}. The Hydrogen Index (HI) is a measure of the potential of the source rock to generate petroleum (Equation (1)). The total amount of CO_2 generated is measured as the S_3 peak (Equation (2)). The Oxygen Index (OI) is the measure of the limitation of CO_2 quantity. Production index (PI) is the ratio of the remnant hydrocarbon

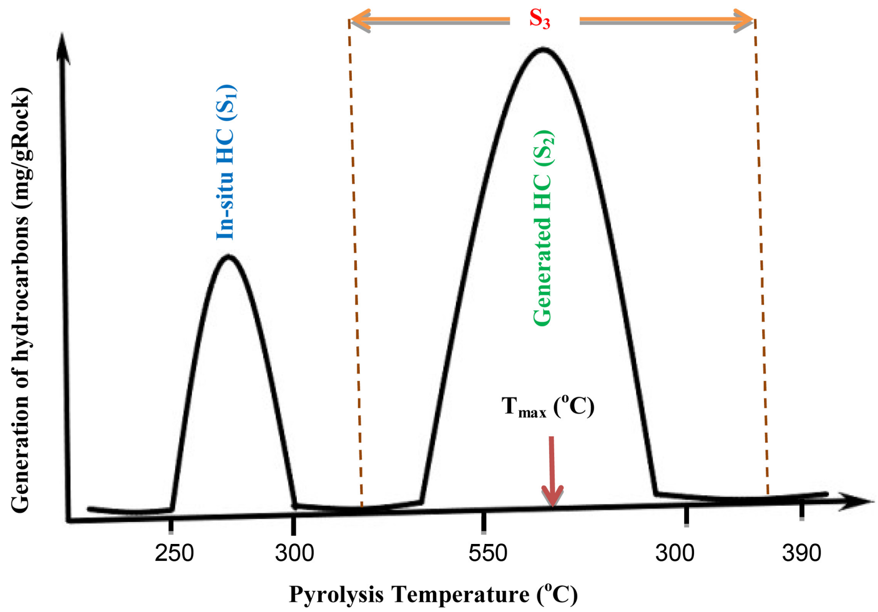

Figure 4. Rock-Eval pyrolysis showing S1, S2, S3, and T_{max} (Modified from Bjorlykke, 2010).

to the total generated (Equation (3)). The higher the value of the production index the better the source rock. The temperature coinciding with maximum hydrocarbon generation is known as T_{max}, which has a typical range 420˚C - 460˚C (**Figure 4**).

$$HI = \frac{S_2}{TOC} \tag{1}$$

$$OI = \frac{S_3}{TOC} \tag{2}$$

$$PI = \frac{S_1}{S_1 + S_2} \tag{3}$$

where HI is the hydrogen index, OI is the oxygen index, PI is the production index, TOC is the total organic carbon, S_1 is the remnant hydrocarbon, S_2 is the generated hydrocarbon, and S_3 quantity of CO_2 formed.

3.1.1. Amount of Organic Matter

The quantity, (amount of organic matter) is commonly assessed by a measure of the total organic carbon (TOC) contained in a rock (Langford & Blanc-Valleron, 1990). Typical source rocks, usually shales or limestones, contain about 1% organic matter and at least 0.5% total organic carbon (TOC), although a rich source rock might have as much as 10% organic matter. The organic richness of rocks is customarily expressed in terms of the percentage by weight of organic carbon (TOC wt %) (Wang et al., 2021). The minimum concentration of organic carbon sufficient enough to saturate the pore network for an adequate level of expulsion efficiency from a potential source rock is 1.0% TOC, although a threshold as low as 0.5% TOC are however considered possible in gas-prone systems which are largely driven by diffusion at an adequate level of the concentration gradient (Asadu et al., 2015). Generally, the amount of TOC in shales (especially black shale) is always higher than five times that of carbonate or other beds of sediments but the potential to generate hydrocarbons from the organic matter is more in carbonate rocks than in shales (Rop & Patwardhan, 2013).

3.1.2. Kerogen Type

Kerogen is a collective name for organic material that is insoluble in organic solvents, water, or oxidizing acids. The portion of the organic material soluble in organic solvents is called bitumen, which is essentially oil in a solid state. With increasing temperature, the chemical bonds in these large molecules (Kerogen) are broken and Kerogen is transformed into smaller molecules that make up oil and gas. This requires that the temperature must be 80˚C - 150˚C over a long geological time (typically 1 - 100 million years). The conversion of Kerogen to oil and gas is thus a process that requires both higher temperatures than one finds at the surface of the earth and a long period of geological time (Pepper & Corvi, 1995). Only when temperatures of about 80˚C - 90˚C are reached, i.e. at 2 - 3 km depth, does the conversion of organic plant and animal matter to hydrocarbons very slowly begin to take place. About 100˚C - 150˚C is the ideal temperature range for this conversion of Kerogen to oil, which is called maturation. This corresponds to a depth of 3 - 4 km with a normal geothermal gradient (about 30˚C - 40˚C/km) (Bjørlykke, 2010). The three possible hydrocarbon source rock facies that may be identified from the seismic geometries include Type I (marine or lacustrine algal Kerogen, oil-prone), Type II (mixed marine and terrestrial organic material, oil and gas-prone), and Type III (terrestrial plant material, gas prone) (Liner & McGilvery, 2019; Tissot & Welte, 1984).

3.1.3. Maturity

A theoretical maturity parameter (P) can be calculated by integrating temperature with respect to time:

$$P = \ln \int_0^t 2^{T/10} \cdot \mathrm{d}T \tag{4}$$

where t, is geological time (million years); T, is the temperature (˚C). We see that a doubling of the reaction rate for every 10˚C is built into this expression (Goff, 1983). The maturity of source rocks can now be calculated with the help of basin modeling integrating temperature over time (Mani et al., 2015). The source rock generative properties such as the T_{max} and Vitrinite reflectance can then be determined. The subsidence curve for the source rock is determined from the stratigraphic age and thickness of the overlying sequence. When the subsidence curve is overlaid with the temperature, transformation ratio, and Vitrinite reflectance, information on the various hydrocarbon windows is obtained ranging from immature to Overmature (Makeen et al., 2016).

3.2. Petroleum System Modeling

A network of mature source rocks, migration channels, reservoir rocks, and trapping and seal rocks in a geologic system constitute petroleum system elements (Ombati et al., 2022). The combination of petroleum system elements and geologic processes such as hydrocarbon generation, migration, and accumulation defines a petroleum system and determines the existence of accumulated hydrocarbon in a given geologic environment (Hantschel & Kauerauf, 2009). Petroleum system models require geochemical and petrophysical characterization of the sedimentary formations in conjunction with boundary conditions that include basal heat flow, sediment-water interface temperature, and Paleo-water depth (Magoon & Dow, 1994) (**Figure 5**). Petroleum systems modeling software is used to integrate all the information at hand to yield a range of scenarios in which the conditions of the petroleum system could have evolved in the past (Busanello et al., 2017). In this study, petroleum system 1D modeling was focused on the play elements' properties through geological time at a well location whereas the petroleum system quick look focused on the spatial distribution of play elements and properties represented as a map.

4. Results and Discussions

The geochemical characteristics: Total organic carbon content (TOC), Vitrinite reflectance (R_0), Kerogen typing, and hydrocarbon content analysis of the sample petroleum source rocks were analyzed. Weatherford laboratories analyzed Kubwa-1 and Mbawa-1 samples, Geotech laboratories did for Pomboo-1, and Simba-1 samples were analyzed by Core laboratories. A total of 254 samples were taken through Rock–Eval pyrolysis consisting of 52 from Mbawa-1, 107 from Simba-1, 64 from Kubwa-1, and 31 from Pomboo-1. The results are presented in **Tables 2-5**.

Table 2 shows the average TOC values for four offshore wells. Kubwa-1 well gave an average TOC of 0.45 wt %, 1.04 wt % for Mbawa-1, 1.20 wt % for Pomboo-1, and 0.91 wt % for Simba-1 well. This gives an average of 0.89 wt % TOC value of the study area indicating a fair organic richness (refer to **Table 1**). When the samples from the late Cretaceous and the Paleogene are compared, the organic richness seems higher in the late Cretaceous (0.98 wt %) than in the Paleocene (0.81 wt %). The range of TOC values per well includes Kubwa-1 (0.09 wt % - 1.27 wt %), Mbawa-1 (0.1 wt % - 1.5 wt %), Pomboo-1 (0.82 wt % - 2.02 wt %), and Simba-1 (0.58 wt % - 2.23 wt %).

Vitrinite reflectance and T_{max} values in the study area range from 0.5% to 0.7% and 304˚C to 444˚C respectively. Simba-1 well shows the highest T_{max} range value compared to the other three wells. The highest Vitrinite reflectance value was obtained in Kubwa-1 well. The results suggest the possible presence of both immature and mature source rocks. Values between 0% to 0.5% Vitrinite reflectance and 300˚C to 430˚C T_{max} correspond to immature source rocks. The oil window will be indicated by Vitrinite reflectance (0.6% - 1.3%) and T_{max} (430˚C - 465˚C) while the gas zone is shown with values of above 1.3% Vitrinite reflectance and above 465˚C T_{max} value. Kubwa-1 and Mbawa-1 T_{max} values suggest a

Table 2. Average source rock TOC values for four offshore wells.

Age	Kubwa-1	Mbawa-1	Pomboo-1	Simba-1	Average
Paleogene	0.51	0.94	1.01	0.78	0.81
Late Cretaceous	0.38	1.13	1.38	1.04	0.98
Early Cretaceous		0.43			
Average	0.45	1.04	1.20	0.91	0.89

Table 3. Geochemical and Rock-Eval pyrolysis data parameters for Kubwa-1 well.

Depth (m)	Formation	T_{max} (˚C)	S_1	S_2	S_3	$S_1 + S_2$	S_2/S_3	PI	TOC	HI	OI	R_o
3330	Miocene	396	0.26	1.01	2.4	1.27	0.4	0.20	0.7	140	333	0.5
3340	Miocene	389	0.12	0.71	1.74	0.83	0.4	0.14	0.8	92	226	0.5
3770	Paleocene	375	0.18	0.77	0.64	0.95	1.2	0.19	1	81	67	0.5
4000	Paleocene	331	0.56	0.72	0.47	1.28	1.5	0.44	1	76	49	0.6
4020	Paleocene		0.51	0.54	0.41	1.05	1.3	0.49	0.9	59	45	0.6
4300	Maastrichtian		0.44	0.59	0.37	1.03	1.6	0.43	0.8	73	46	0.6
4350	Maastrichtian	419	0.54	0.95	1.01	1.49	0.9	0.36	1.1	87	93	0.7
4354	Maastrichtian	437	0.13	0.74	0.33	0.87	2.2	0.15	1.1	66	29	0.7
4400	Maastrichtian	418	0.29	0.66	0.77	0.95	0.9	0.31	1.3	52	61	0.7
4790	Maastrichtian	428	0.17	0.68	0.35	0.85	1.9	0.20	0.8	88	45	0.7

lack of a mature source rock or limited mature source rock whereas in Pomboo-1 and Simba-1 there is a likelihood of having a mature source rock given the T_{max} values obtained.

In measuring the quality of the organic matter in the various formation samples within the study area, Kerogen typing was performed using TOC and Rock-Eval pyrolysis (**Figure A1**) (Steiner et al., 2016). Type III Kerogen was found to be the most dominant Kerogen type, and gas shows are the most frequent hydrocarbon encountered in the Lamu Basin (**Figure 3**). The hydrogen index (HI) range for the studied wells is 52 to 140 mg HC/g TOC (Kubwa-1), 3 to 141 mg HC/g TOC (Mbawa-1), 244 to 608 mg HC/g TOC (Pomboo-1), and 4 to 274 mg HC/g TOC (Simba-1). HI values below 200 mg HC/g TOC suggest type III Kerogen which is gas-prone. Type II/III Kerogen (Oil/gas-prone) is suggested by the HI values between 200 mg HC/g TOC to 300 mg HC/g TOC. Oil-prone type II Kerogen is suggested by the HI values above 300 mg HC/g TOC. The oxygen index (OI) ranges from 21 mg HC/g TOC to 1241 mg HC/g TOC in the four wells. This negatively correlates with TOC (Arab et al., 2015). The higher the value of the production index (PI), the better the source rock (Ratnayake et al., 2018). The PI range in the four wells is from 0.1 to 0.93, the

Table 4. Geochemical and rock-eval pyrolysis data parameters for Mbawa-1.

Depth (m)		Formation	T_{max}	Leco	RE			(S1/TOC) *100	S_2/S_3	HI	OI	PI	Ro, %
Top	Bottom		(˚C)	TOC	S_1	S_2	S_3						
1519	1520	Lower Eocene	−1	0.2	0.02	0.01	0.46	10	0.0	5	232	0.67	
1520	1530	Lower Eocene	−1	0.3	0.01	0.01	0.41	3	0.0	3	136	0.50	
1530	1550	Lower Eocene	353	0.7	0.06	0.32	1.94	9	0.2	49	298	0.16	
1550	1580	Upper Paleocene	−1	0.4	0.02	0.04	0.49	5	0.1	10	124	0.33	
1580	1610	Middle Paleocene	−1	0.2	0.02	0.06	0.57	9	0.1	28	263	0.25	
1610	1640	Middle Paleocene	−1	1.2	0.01	0.04	0.59	1	0.1	3	51	0.20	
1640	1670	Lower Paleocene	422	0.8	0.02	0.04	0.54	2	0.1	5	68	0.33	
1670	1700	Upper Maastrichtian	334	0.6	0.01	0.03	0.58	2	0.1	5	101	0.25	
1700	1730	Upper Maastrichtian	422	0.7	0.02	0.07	0.49	3	0.1	10	70	0.22	
1730	1760	Lower Maastrichtian	359	0.8	0.04	0.08	0.47	5	0.2	9	55	0.33	
1760	1790	Lower Maastrichtian	−1	0.6	0.03	0.05	0.47	5	0.1	8	76	0.38	
1790	1820	Upper Campanian	316	0.9	0.04	0.13	0.36	4	0.4	14	40	0.23	
1820	1850	Upper Campanian	364	0.7	0.10	0.11	0.67	14	0.2	15	91	0.48	
1850	1880	Upper Campanian	327	0.9	0.04	0.17	0.27	5	0.6	20	31	0.19	
1880	1910	Upper Campanian	428	1.1	0.05	0.26	0.51	5	0.5	24	47	0.16	
1910	1940	Upper Campanian	435	1.5	0.05	0.42	0.52	3	0.8	28	34	0.11	
1940	1970	Upper Campanian	426	1.5	0.06	0.45	0.5	4	0.9	30	33	0.12	
1970	2000	Upper Campanian	431	1.5	0.05	0.44	0.34	3	1.3	29	23	0.10	
2000	2006	Upper Campanian	427	1.2	0.04	0.3	0.25	3	1.2	25	21	0.12	
2006	2030	Upper Campanian	426	1.0	0.05	0.33	0.34	5	1.0	33	34	0.14	
2030	2060	Upper Campanian	425	0.8	0.04	0.18	0.36	5	0.5	22	44	0.18	
2060	2083	Upper Campanian	361	0.3	0.02	0.07	0.38	6	0.2	20	111	0.22	
2083	2086	Upper Campanian	−1	0.3	0.04	0.07	0.48	12	0.1	22	148	0.37	
2086	2089	Upper Campanian	429	0.8	0.10	0.33	0.7	12	0.5	39	83	0.23	
2089	2092	Upper Campanian	318	0.3	0.07	0.07	0.32	21	0.2	21	94	0.51	
2092	2095	Upper Campanian	304	0.4	0.06	0.16	0.22	14	0.7	36	50	0.27	
2095	2098	Upper Campanian	−1	0.2	0.00	0.01	0.11	−1	0.1	6	61	−1.00	
2098	2101	Upper Campanian	338	0.2	0.05	0.03	0.47	30	0.1	18	281	0.63	
2101	2104	Upper Campanian	361	0.4	0.14	0.29	1.07	37	0.3	75	278	0.33	
2104	2107	Upper Campanian	423	0.5	0.24	0.71	1.05	49	0.7	141	209	0.26	
2107	2110	Upper Campanian	324	0.5	0.06	0.16	0.3	11	0.5	31	58	0.27	
2110	2113	Upper Campanian	−1	0.3	0.06	0.05	0.33	24	0.2	20	129	0.55	

Continued

2113	2116	Upper Campanian	422	0.2	0.04	0.07	0.57	19	0.1	32	263	0.37
2116	2119	Upper Campanian	−1	0.3	0.04	0.04	0.62	14	0.1	14	219	0.50
2119	2122	Upper Campanian	423	0.3	0.06	0.13	0.72	21	0.2	47	259	0.31
2122	2125	Upper Campanian	366	0.4	0.09	0.15	0.74	21	0.2	35	172	0.37
2125	2128	Upper Campanian	346	0.4	0.06	0.12	0.76	15	0.2	30	190	0.34
2128	2131	Middle Campanian	−1	0.2	0.10	0.04	0.75	54	0.1	22	410	0.71
2131	2134	Middle Campanian	−1	0.1	0.06	0.04	0.56	79	0.1	53	747	0.60
2134	2137	Middle Campanian	−1	0.1	0.02	0.01	0.41	29	0.0	14	577	0.67
2137	2140	Middle Campanian	−1	0.0	0.02	0.01	0.36	69	0.0	34	1241	0.67
2140	2143	Middle Campanian	−1	0.1	0.01	0.01	0.26	16	0.0	16	413	0.51
2143	2146	Middle Campanian	−1	0.3	0.02	0.02	0.42	8	0.0	8	167	0.51
2146	2149	Middle Campanian	−1	0.0	0.02	0.01	0.38	49	0.0	24	927	0.67
2149	2152	Middle Campanian	−1	0.1	0.00	0.01	0.68	−1	0.0	7	493	−1.00
2152	2155	Lower Campanian	366	0.2	0.18	0.06	1.12	111	0.1	36	675	0.75
2155	2158	Lower Campanian	−1	0.1	0.10	0.04	0.84	99	0.0	40	848	0.71
2158	2161	Lower Campanian	338	0.4	0.13	0.1	0.89	37	0.1	29	254	0.56
2161	2164	Lower Campanian	428	0.6	0.10	0.24	0.63	18	0.4	42	109	0.30
2164	2167	Lower Campanian	422	0.7	0.17	0.5	1.23	25	0.4	74	182	0.25
2167	2173	Lower Campanian	422	0.3	0.10	0.15	0.74	40	0.2	58	287	0.41
2173	2179	Lower Campanian	320	0.3	0.09	0.1	0.73	30	0.1	32	235	0.48
2179	2185	Lower Campanian	−1	0.2	0.07	0.05	0.84	32	0.1	23	378	0.59
2185	2191	Lower Campanian	426	0.6	0.09	0.18	0.58	16	0.3	32	104	0.33
2191	2197	Lower Campanian	314	0.1	0.07	0.04	0.67	100	0.1	57	957	0.64
2197	2203	Lower Campanian	353	0.3	0.13	0.13	0.83	43	0.2	42	269	0.50
2203	2227	Upper Santonian	−1	0.1	0.00	0.02	0.46	−1	0.0	19	434	−1.00
2227	2260	Upper Santonian	−1	0.2	0.04	0.04	0.56	23	0.1	23	316	0.50
2260	2290	Middle Santonian	407	0.1	0.05	0.04	0.68	35	0.1	28	476	0.56
2290	2323	Lower Santonian	−1	0.2	0.05	0.04	0.64	31	0.1	25	398	0.56
2323	2353	Lower Santonian	−1	0.2	0.06	0.05	0.79	31	0.1	26	409	0.54
2353	2383	Upper Turonian	−1	0.2	0.07	0.11	0.64	40	0.2	62	364	0.39
2383	2413	Middle Turonian	318	0.1	0.05	0.04	0.55	41	0.1	32	444	0.56
2413	2443	Middle Turonian	315	0.2	0.05	0.04	0.58	33	0.1	26	379	0.56
2443	2475	Middle Turonian	422	0.2	0.07	0.07	0.68	42	0.1	41	400	0.51
2475	2505	Middle Turonian	345	0.2	0.08	0.06	0.68	33	0.1	25	282	0.57

Continued

2505	2535	Lower Turonian	−1	0.2	0.07	0.04	0.78	33	0.1	18	358	0.64
2535	2553	Lower Turonian	−1	0.3	0.06	0.07	0.58	20	0.1	22	184	0.47
2553	2580	Lower Turonian	−1	0.4	0.09	0.07	0.58	21	0.1	17	137	0.56
2580	2610	Lower Turonian	−1	0.5	0.12	0.07	0.54	25	0.1	15	113	0.63
2610	2640	Upper Cenomanian	−1	0.5	0.18	0.12	0.59	37	0.2	24	118	0.61
2640	2670	Upper Cenomanian	−1	0.3	0.07	0.07	0.52	28	0.1	27	202	0.50
2670	2700	Middle Cenomanian	−1	0.4	0.10	0.07	0.67	26	0.1	18	171	0.59
2700	2730	Middle Cenomanian	−1	0.2	0.04	0.02	0.57	25	0.0	12	341	0.67
2730	2760	Middle Cenomanian	−1	0.2	0.13	0.19	0.66	64	0.3	93	324	0.41
2760	2790	Middle Cenomanian	−1	0.2	0.09	0.14	0.72	52	0.2	81	419	0.39
2790	2820	Middle Cenomanian	423	0.2	0.08	0.16	0.66	44	0.2	86	357	0.34
2820	2850	Middle Cenomanian	311	0.3	0.11	0.21	0.72	42	0.3	80	274	0.34
2850	2880	Upper Albian	422	0.3	0.09	0.13	1.03	26	0.1	38	299	0.41
2880	2910	Upper Albian	351	0.4	0.12	0.16	1.27	27	0.1	36	286	0.43
2910	2940	Upper Albian	413	0.3	0.12	0.24	0.95	40	0.3	80	317	0.34
2940	2970	Upper Albian	−1	0.3	0.10	0.15	0.76	31	0.2	46	231	0.41
2970	3000	Upper Albian	−1	0.2	0.11	0.16	0.72	48	0.2	70	317	0.41
3000	3030	Upper Albian	355	0.3	0.31	0.36	0.46	95	0.8	112	143	0.46
3030	3060	Upper Albian	−1	0.2	0.13	0.15	0.68	53	0.2	62	280	0.46
3060	3090	Middle Albian	−1	0.3	0.13	0.11	0.7	45	0.2	38	241	0.54
3090	3120	Middle Albian	−1	0.2	0.10	0.11	0.67	41	0.2	45	272	0.48
3120	3150	Middle Albian	−1	0.2	0.05	0.06	0.86	29	0.1	34	494	0.45

smallest value obtained from Mbawa-1 well and the highest from Simba-1 well.

Petroleum system modeling was applied in evaluating geological conditions necessary for a successful charge. The three major stages involved in petroleum system modeling include the making model stage, the numerical simulation stage, and the calibration/inferences stage (**Figure 5**). Schlumberger's Petrel 2017 software was used in petroleum system modeling.

Figure 6(a), **Figure 7(a)**, and **Figure 8(a)** show the highest temperature (246.56˚C), transformation ratio (99.19%), and Vitrinite reflectance (3.0) in Kubwa-1 respectively. This is achieved at the Cretaceous (Maastrichtian) time at a depth of about 4500 m. The transformation ratio curve indicates both mature and immature source rocks where generation with/without expulsion has occurred in the cretaceous and no generation in the rest of the time. The Vitrinite reflectance curve indicates Overmature Cretaceous (Maastrichtian), gas generation in Paleocene, and oil window during the Miocene.

Table 5. Geochemical and Rock-Eval pyrolysis data parameters for Pomboo-1.

Depth (m)	Formation	T_{max} (˚C)	S_1	S_2	S_3	$S_1 + S_2$	S_2/S_3	PI	TOC	HI	OI	R_o
2950	Middle Eocene	441	1.47	3.93	2.91	5.4	1.35	0.27	0.82	479	356	
3040	Middle-Early Eocene	419	1.06	3.17	2.23	4.23	1.42	0.25	0.89	356	252	
3140	Middle-Early Eocene	367	2.39	3.47	2.16	5.86	1.61	0.41	0.94	369	230	
3170	Early Eocene	360	3.92	3.64	1.93	7.56	1.89	0.52	1.07	340	180	
3270	Late Paleocene	426	3.16	4.42	2.22	7.58	1.99	0.42	1.3	340	171	
3340	Late Maastrichtian	427	9.16	8.08	2.16	17.24	3.74	0.53	2.02	400	107	
3420	Late Maastrichtian	388	3.87	2.76	1.76	6.63	1.57	0.58	1.13	244	156	
3480	Late Maastrichtian	428	5.29	4.88	1.62	10.17	3.01	0.52	1.47	332	110	
3530	Late Maastrichtian	430	3.23	5.22	1.4	8.45	3.73	0.38	1.32	395	106	
3650	Late Maastrichtian	426	1.4	4.84	1.66	6.24	2.92	0.22	1.13	428	147	
3790	Late Maastrichtian	426	2.75	4.97	1.59	7.72	3.13	0.36	1.15	432	138	
3830	Late Maastrichtian	428	2.8	5.44	1.37	8.24	3.97	0.34	1.3	418	105	
3900	Early Maastrichtian	425	6.28	6.16	1.95	12.44	3.16	0.5	1.88	328	104	
3990	Early Maastrichtian	429	4.65	7.02	1.82	11.67	3.86	0.4	1.6	439	114	
4040	Early Maastrichtian	430	1.52	2.72	1.7	4.24	1.6	0.36	0.92	296	185	
4140	Early Maastrichtian	431	3.69	6.08	2.04	9.67	2.98	0.37	1.44	422	142	
4190	Early Maastrichtian	426	6.04	5.32	1.59	11.36	3.35	0.53	1.53	348	104	0.58
4210	Early Maastrichtian	429	1.98	4.44	1.6	6.42	2.78	0.31	1.23	361	130	
4230	Early Maastrichtian	428	5.58	6.78	1.94	11.36	3.5	0.49	1.54	375	107	
4270	Early Maastrichtian	425	7.64	6.16	1.6	13.8	3.85	0.55	1.69	364	95	
4300	Early Maastrichtian	424	4.44	4.23	1.92	8.67	2.2	0.51	1.33	318	144	
4320	Early Maastrichtian	428	5.16	4.72	1.77	9.88	2.67	0.52	1.43	330	124	
4390	Early Maastrichtian	429	5.7	6.08	1.95	11.78	3.12	0.48	1.64	371	119	0.6
4420	Early Maastrichtian	430	4.9	7.22	2.18	12.12	3.31	0.4	1.74	415	125	
4430	Early Maastrichtian	419	6.62	5	1.85	11.62	2.7	0.57	1.65	303	112	
4470	Early Maastrichtian	426	5.8	6.26	2.05	12.06	3.05	0.48	1.66	377	123	
4490	Early Maastrichtian	424	1.31	4.04	1.95	5.35	2.07	0.24	0.99	408	197	0.61
4520	Late Campanian	426	1	4.22	1.91	5.22	2.21	0.19	1.02	414	187	
4540	Late Campanian	422	1.72	4.28	1.8	6	2.38	0.29	0.84	510	214	
4590	Late Campanian	427	1.17	5.16	1.95	6.33	2.65	0.18	1.02	506	191	0.68
4610	Late Campanian	433	1.21	6.32	2.64	6.53	2.39	0.19	1.04	512	214	0.62

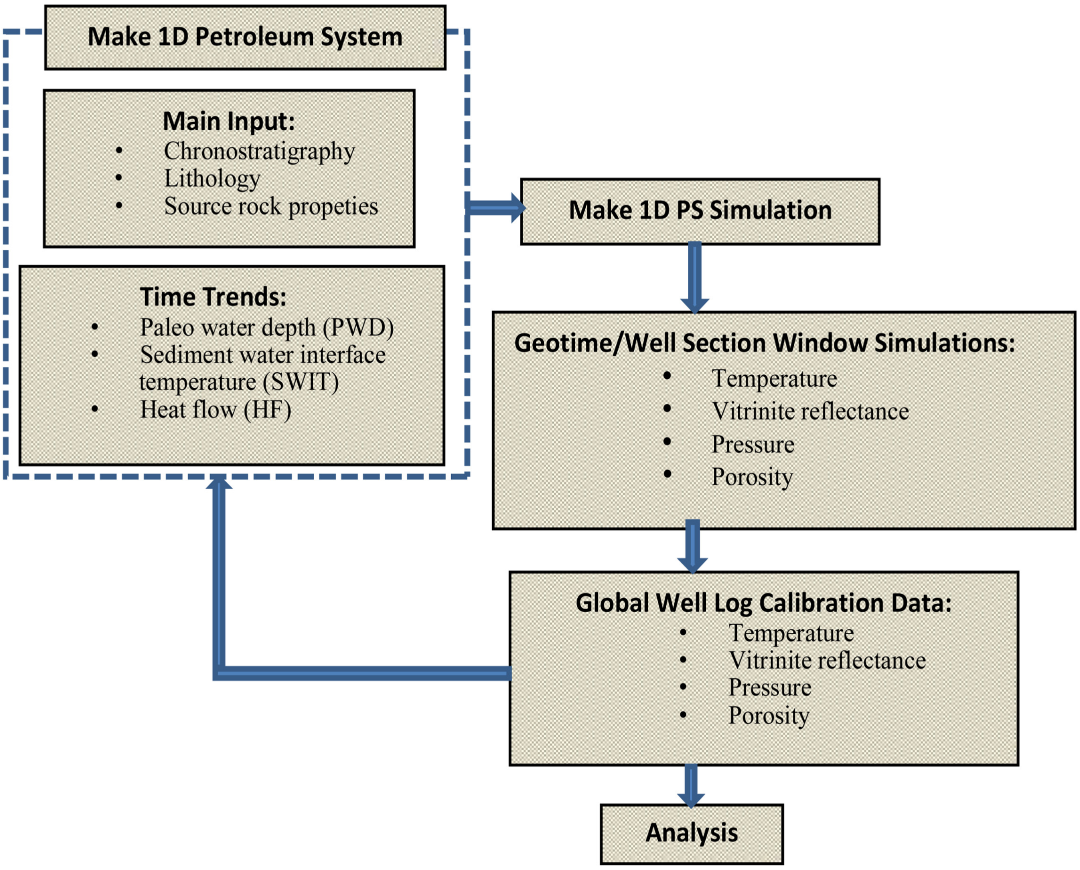

Figure 5. 1D petroleum system modeling workflow (modified from Schlumberger modules).

Figure 6(b) shows the highest temperature of 109.81˚C achieved between the bases Campanian and base Paleocene at a depth of between 1800 m and 2300 m for the Mbawa-1 well. The maximum transformation ratio value in Figure 7(b) is 47.94% which signifies a possible oil generation at the base Campanian but without an expulsion. Figure 8(b) is the Vitrinite reflectance curve with a reading of 0.7 implying an early oil window at the base Paleocene and base Campanian.

Figure 6(c), Figure 7(c), and Figure 8(c) show 158.13˚C as the highest temperature achieved during the base Campanian at a depth of over 2600 m, more than 50% transformation ratio at a depth of between 2500 m to 4000 m, and Vitrinite reflectance value of between 0.5% and more than 2.0% for Pomboo-1 well respectively. The Vitrinite reflectance curve suggests a possible gas generation window during the base Campanian and an oil window between the base Eocene and the base Campanian.

Figure 6(d), Figure 7(d), and Figure 8(d) are the standard interpretation scales for temperature, transformation ratio, and Vitrinite reflectance respectively. The temperature scale shows diagenesis happening below 50˚C whereby only biogenic gas may be generated. The hydrocarbon is said to be immature since this corresponds to a T_{max} value below 430˚C. Catagenesis follows at a temperature between 50˚C - 200˚C corresponding to T_{max} (430˚C - 550˚C)

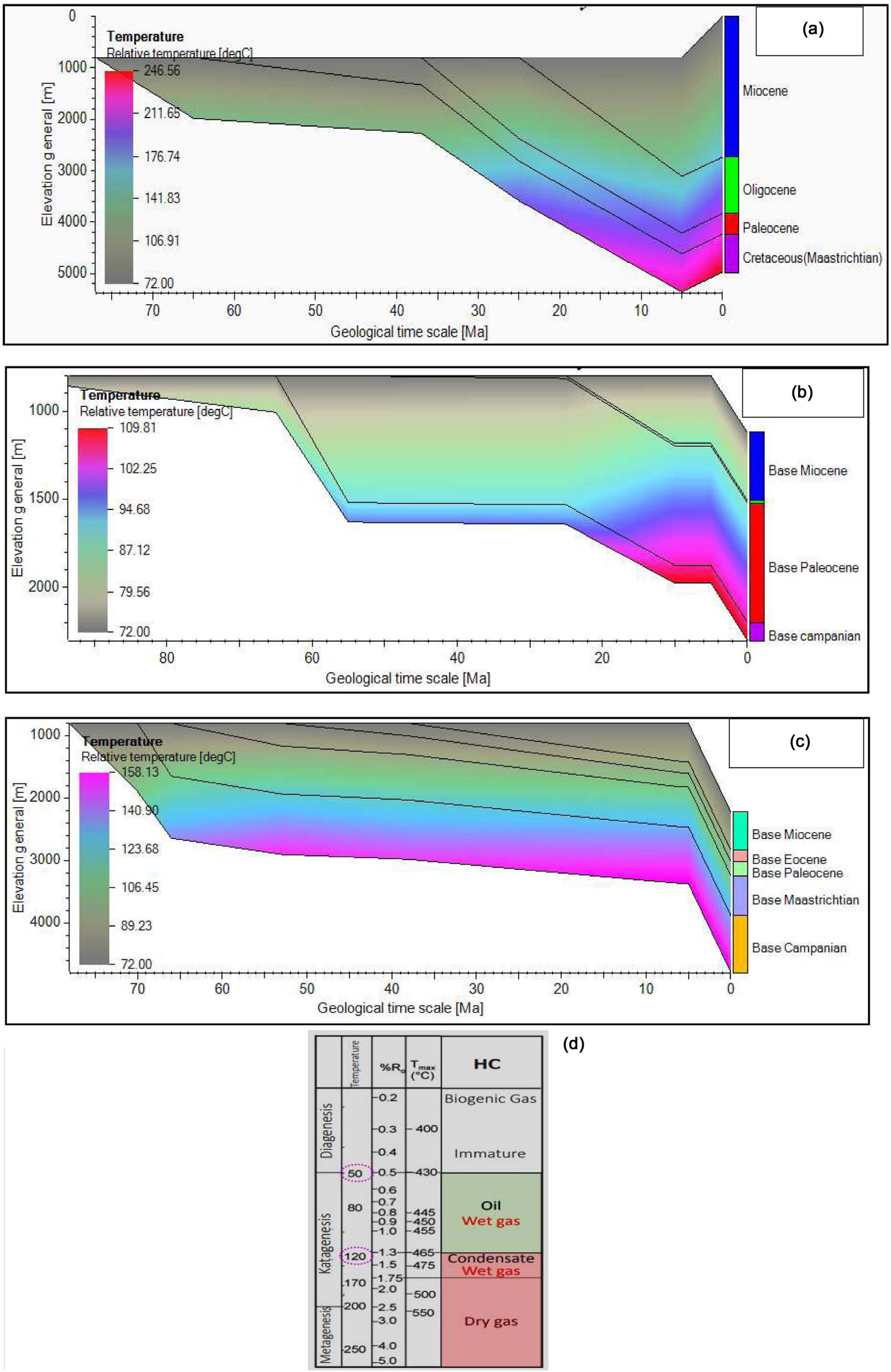

Figure 6. Burial curve overlayed with the relative temperature for (a) Kubwa-1 (b) Mbawa-1 (c) Pomboo-1 (d) Interpretation scale.

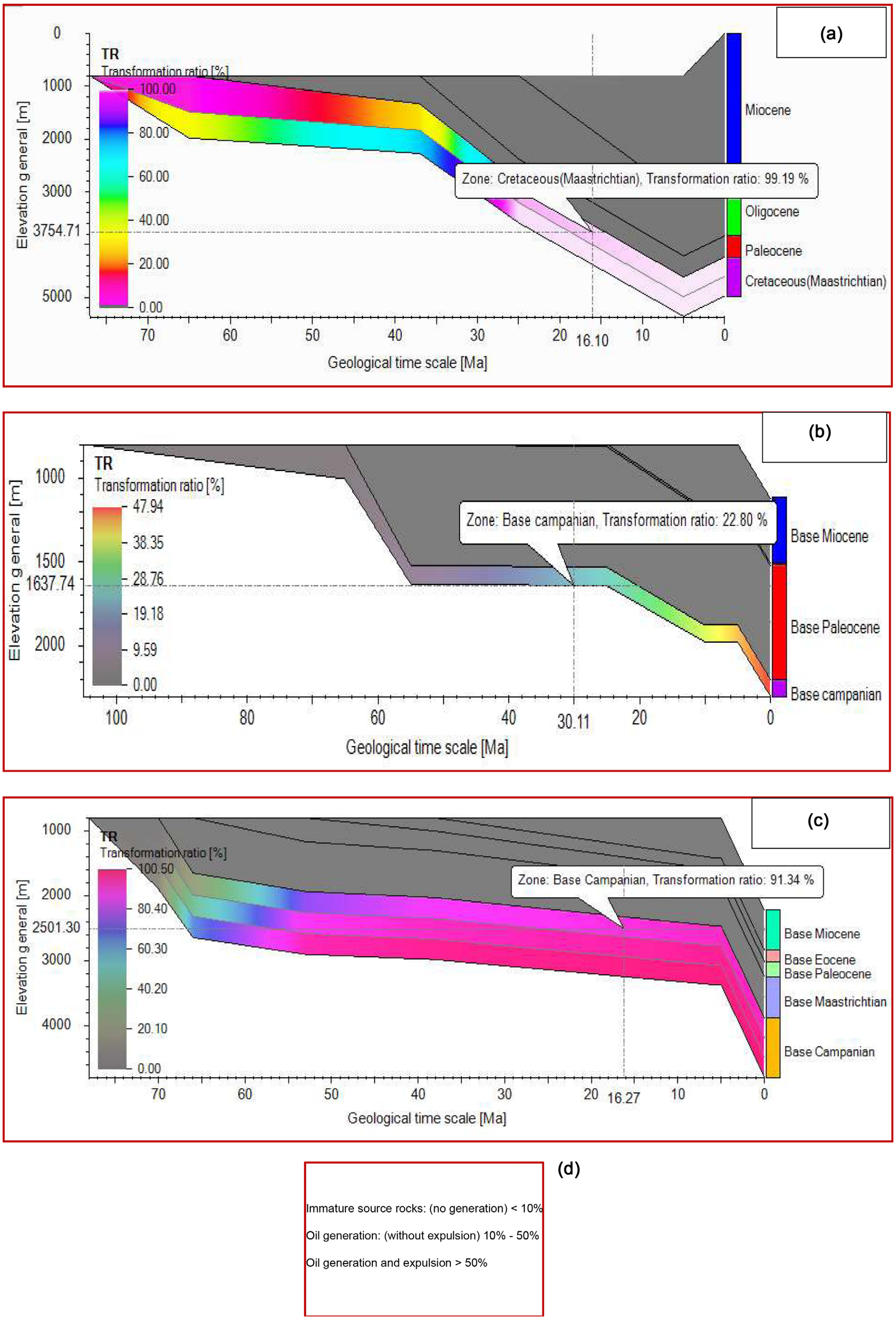

Figure 7. Burial curve overlayed with the transformation ratio for (a) Kubwa-1 (b) Mbawa-1 (c) Pomboo-1 (d) Interpretation scale.

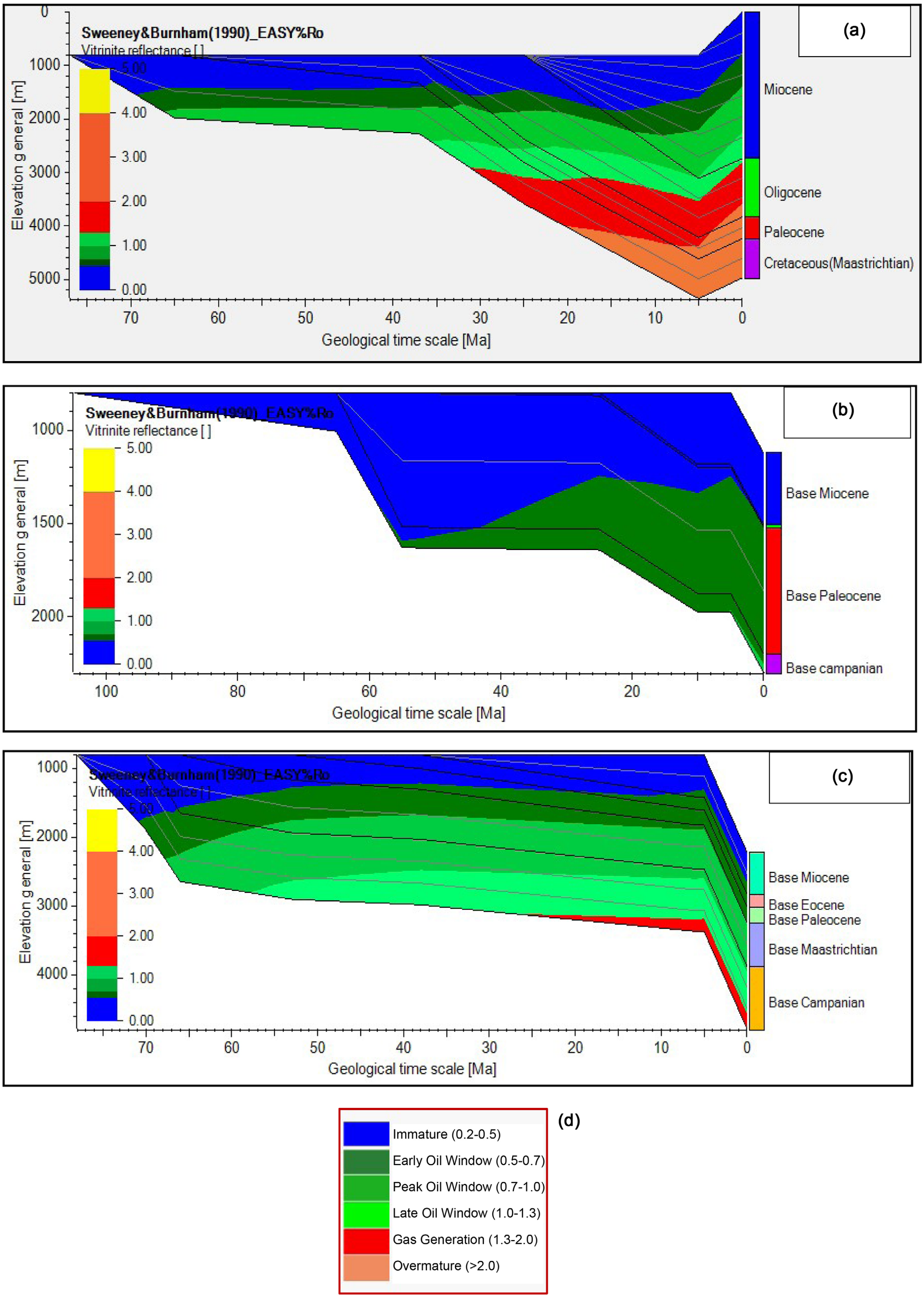

Figure 8. Burial curve overlayed with the Vitrinite reflectance for (a) Kubwa-1 (b) Mbawa-1 (c) Pomboo-1 (d) Interpretation scale.

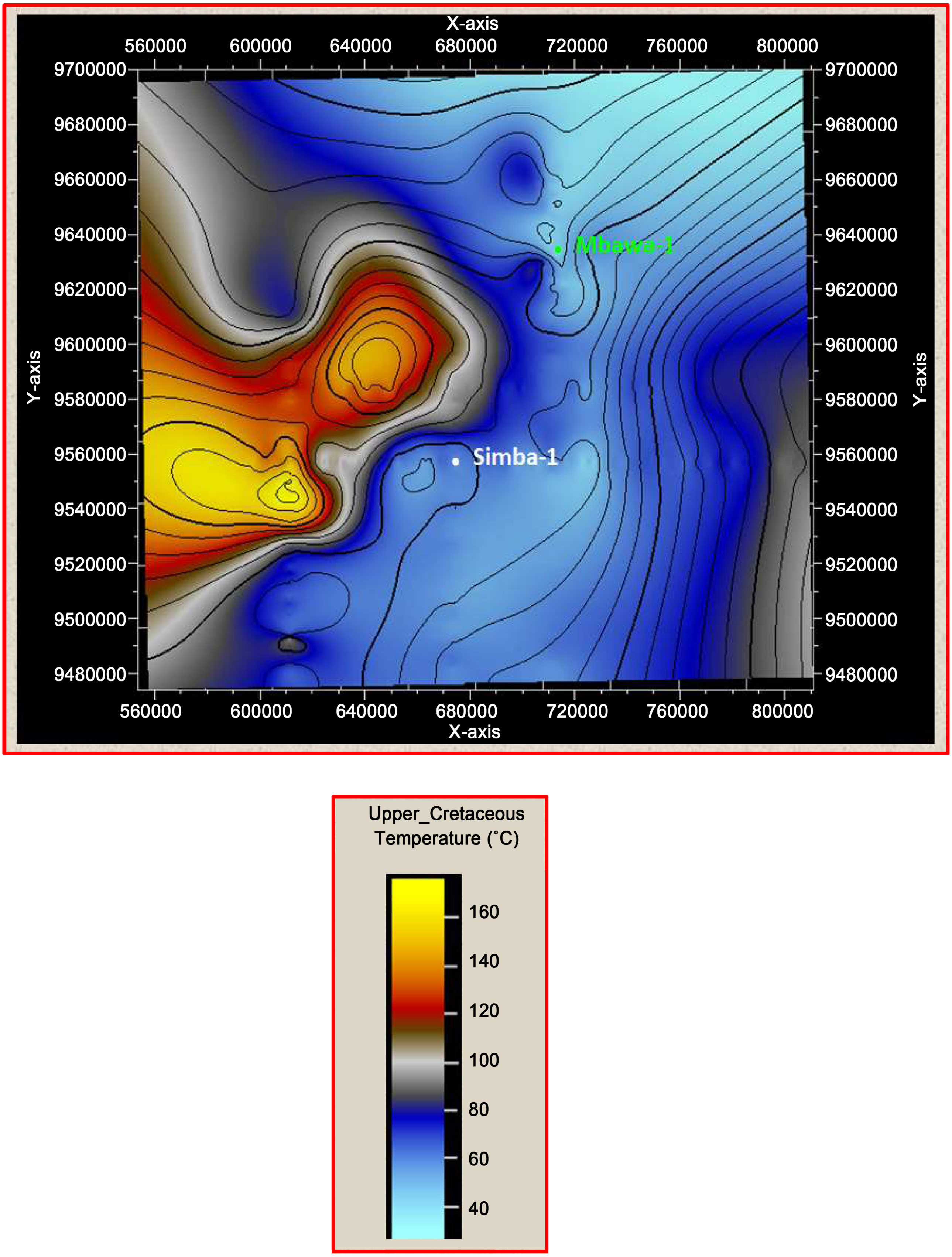

Figure 9. Temperature map. Temperature is still cool towards deep offshore, favorable towards the coastline.

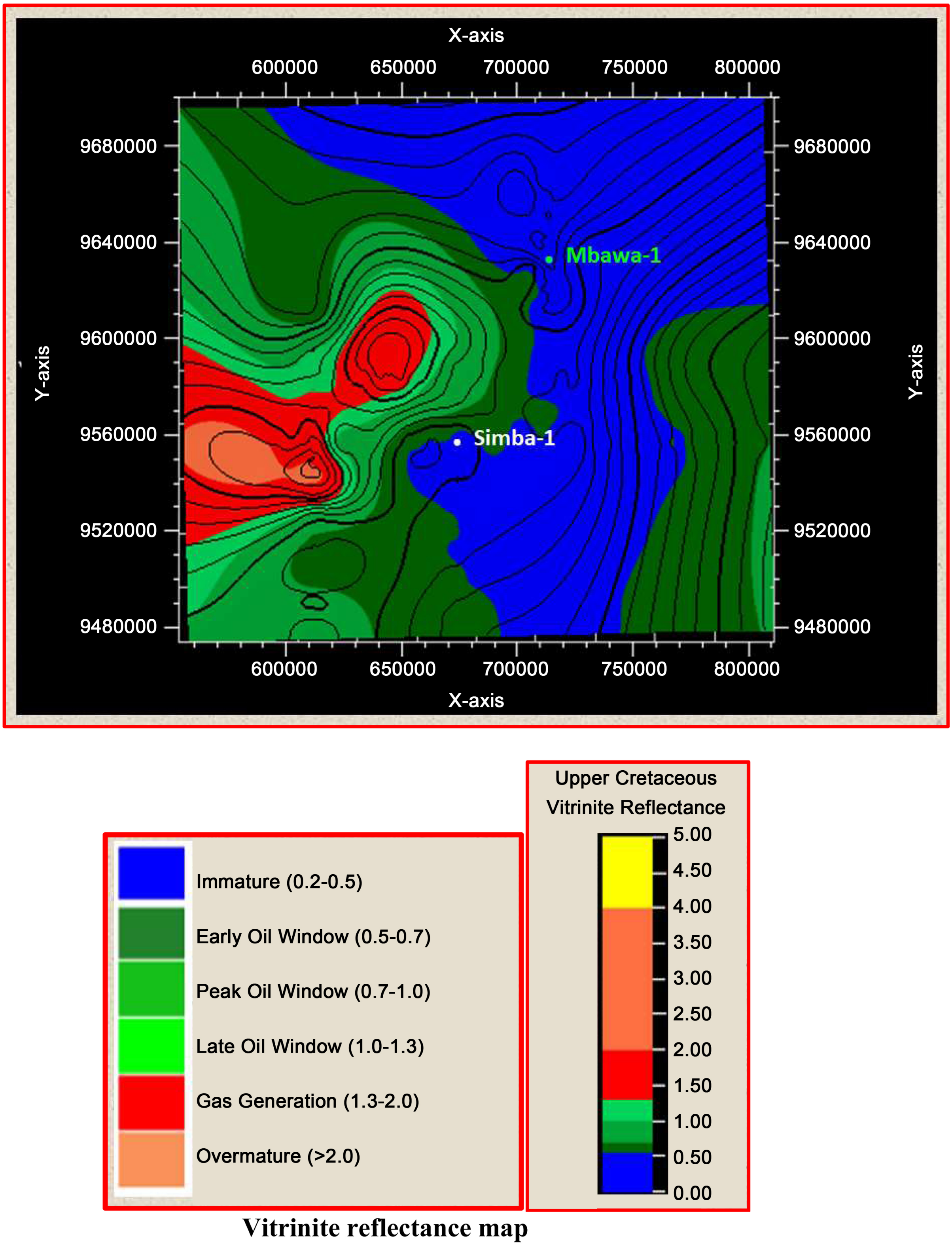

Figure 10. Vitrinite reflectance map.

showing oil and wet gas. Beyond 200˚C temperature (T_{max} > 550˚C) metagenesis sets in showing dry gas. The transformation scale indicates three levels: less than

10% value signifying immature source rock which has not been generated yet, between 10% to 50% the oil generation without expulsion level, and more than 50% value being the oil generation and expulsion level. The Vitrinite reflectance scale shows the immature window (0.2% - 0.5%), early oil window (0.5% - 0.7%), peak oil window (0.7% - 1.0%), late oil window (1.0% - 1.3%), gas generation window (1.3% - 2.0%), and Overmature window (>2.0%).

Figure 9 and Figure 10 are the petroleum system quick-look upper cretaceous surface maps showing the spatial distribution of temperature and Vitrinite reflectance. The maps indicate the region that is favorable for source maturation and maturity status. The region toward the coastline shows higher temperatures compared to regions towards the deep offshore. Since temperature is a factor in source rock maturation, the vitrine reflectance is equally higher near the coastline than the rest of the other regions, especially towards deep offshore. Towards the coastline, there is the early oil window to the Overmature window, whereas towards deep offshore there is the majorly immature window. These results may explain why Pomboo-1, Kubwa-1, and Simba-1 wells were dry, although the Mbawa-1 well had gas shows in the upper cretaceous sandstones.

5. Conclusion

The shallow Lamu offshore source rock quantity, quality, and maturity have been estimated through the determination of the TOC average values, Kerogen typing, and Rock-Eval pyrolysis measurements respectively. The results postulate the absence of a definitive effective source rock with a likelihood of having cases of potential and possible source rocks. The average TOC of 0.89 wt % in the study area suggests a fair organic richness which seems higher in the late cretaceous (0.98 wt %) than in the Paleocene (0.81 wt %). Vitrinite reflectance and T_{max} values in the study area indicate the possible presence of both mature and immature source rocks. For instance, the result implies that Mbawa-1 formation may have not reached the required levels of maturity to begin generating despite the non-commercial gas shown in the upper cretaceous. Type III Kerogen was the most dominant Kerogen type, and gas shows are the most frequent hydrocarbon encountered in the Lamu Basin with a few cases registering type II/III and type II. The charge properties (i.e. Temperature, transformation ratio, and Vitrinite reflectance) over geologic time at each of the three wells have been estimated and their spatial variation mapped as seen from the burial history and depth curves overlaid with temperature, transformation ratio, and Vitrinite reflectance respectively. From the upper cretaceous maturity maps, the results seem to favor near coastal regions where average TOC is about 1.4 wt %, Vitrinite reflectance is more than 0.5%, transformation ratio is more than 10%, and temperatures range from 80˚C to 160˚C. However, greater uncertainty rests on the source rock's presence and viability tending toward the deep offshore. Geochemical analysis and petroleum system modeling for hydrocarbon source rock evaluation improved the understanding of the occurrence of the possible and potential source rocks and processes necessary for hydrocarbon generation.

Acknowledgements

Special thanks to the National Oil Corporation of Kenya (NOCK) for providing the necessary data and allowing me to access the required software in their workstations.

Conflicts of Interest

The authors declare no conflicts of interest regarding the publication of this paper.

References

Al-Areeq, N. M. (2018). Petroleum Source Rocks Characterization and Hydrocarbon Generation. In M. Zoveidavianpoor (Ed.), *Recent Insights in Petroleum Science and Engineering* (p. 1). IntechOpen. https://doi.org/10.5772/intechopen.70092

Al-Hajeri, M. M., Al Saeed, M., Derks, J., Fuchs, T., Hantschel, T., Kauerauf, A., & Tessen, N. (2009). Basin and Petroleum System Modeling. *Oilfield Review, 21,* 14-29.

Arab, M., Bracene, R., Roure, F., Zazoun, R. S., Mahdjoub, Y., & Badji, R. (2015). Source Rocks and Related Petroleum Systems of the Chelif Basin, (Western Tellian Domain, North Algeria). *Marine and Petroleum Geology, 64,* 363-385. https://doi.org/10.1016/j.marpetgeo.2015.03.017

Asadu, A., Omo-Irabor, O., & Ibe, K. (2015). *Source Rock Characterisation of AGBADA Formation in Well Z, Offshore, Niger Delta, Nigeria*.

Bjorlykke, K. (2010). *Petroleum Geoscience: From Sedimentary Environments to Rock Physics*. Springer Science & Business Media. https://doi.org/10.1007/978-3-642-02332-3

Bjørlykke, K. (2010). Sequence Stratigraphy, Seismic Stratigraphy and Basin Analysis. In K. Bjorlykke (Ed.), *Petroleum Geoscience* (pp. 235-251). Springer. https://doi.org/10.1007/978-3-642-02332-3_8

Busanello, G., Del Ben, A., & Pipan, M. (2017). Petroleum Systems Modeling as an Exploration Tool: From Surface Seismic Acquisition to Basin Modeling: A Case Study from a Periplatform Basin in Northern Adriatic. *First Break, 35*. https://doi.org/10.3997/1365-2397.35.3.87564

Coffin, M. F., & Rabinowitz, P. D. (1987). Reconstruction of Madagascar and Africa: Evidence from the Davie Fracture Zone and Western Somali Basin. *Journal of Geophysical Research: Solid Earth, 92,* 9385-9406. https://doi.org/10.1029/JB092iB09p09385

Goff, J. (1983). Hydrocarbon Generation and Migration from Jurassic Source Rocks in the E Shetland Basin and Viking Graben of the Northern North Sea. *Journal of the Geological Society, 140,* 445-474. https://doi.org/10.1144/gsjgs.140.3.0445

Hantschel, T., & Kauerauf, A. I. (2009). *Fundamentals of Basin and Petroleum Systems Modeling*. Springer Science & Business Media.

Hunt, J. M., Philp, R. P., & Kvenvolden, K. A. (2002). Early Developments in Petroleum Geochemistry. *Organic Geochemistry, 33,* 1025-1052. https://doi.org/10.1016/S0146-6380(02)00056-6

Katz, B. J. (1983). Limitations of "Rock-Eval" Pyrolysis for Typing Organic Matter. *Organic Geochemistry, 4,* 195-199. https://doi.org/10.1016/0146-6380(83)90041-4

Kimburi, E., Osicki, O., Rathee, D., Kornpihl, K., & Wanjala, E. (2015). Tectonic Control upon Sedimentation in the Lamu Basin, Kenya. In *The First EAGE Eastern Africa Petroleum Geoscience Forum* (pp. 1-5). European Association of Geoscientists & Engineers. https://doi.org/10.3997/2214-4609.201414451

Langford, F., & Blanc-Valleron, M.-M. (1990). Interpreting Rock-Eval Pyrolysis Data Using Graphs of Pyrolizable Hydrocarbons vs. Total Organic Carbon. *AAPG Bulletin, 74,* 799-804. https://doi.org/10.1306/0C9B238F-1710-11D7-8645000102C1865D

Liner, C. L., & McGilvery, T. A. (2019). *The Art and Science of Seismic Interpretation*. Springer. https://doi.org/10.1007/978-3-030-03998-1

Magoon, L., & Dow, W. (1994). *The Petroleum System: From Source to Trap: AAPG Memoir 60* (pp. 25-49). American Association of Petroleum Geologists, Tulsa. https://doi.org/10.1306/M60585

Makeen, Y. M., Abdullah, W. H., Pearson, M. J., Hakimi, M. H., Elhassan, O. M., & Hadad, Y. T. (2016). Thermal Maturity History and Petroleum Generation Modeling for the Lower Cretaceous Abu Gabra Formation in the Fula Sub-Basin, Muglad Basin, Sudan. *Marine and Petroleum Geology, 75,* 310-324. https://doi.org/10.1016/j.marpetgeo.2016.04.023

Mani, D., Patil, D., Dayal, A., & Prasad, B. (2015). Thermal Maturity, Source Rock Potential and Kinetics of Hydrocarbon Generation in Permian Shales from the Damodar Valley Basin, Eastern India. *Marine and Petroleum Geology, 66,* 1056-1072. https://doi.org/10.1016/j.marpetgeo.2015.08.019

Ngechu, J. M. (2012). *Assessment of Source Rock Maturity in the Lamu Basin Based on Well Distribution, Hydrocarbon Shows, Total Organic Carbon (TOC) Levels, Kerogen Type, and Vitrinite Reflectance.* University of Nairobi, Kenya.

NOCK (1995). *Hydrocarbon Potential of the Coastal Onshore and Offshore Lamu Basin of Southeast Kenya* (p. 97). NOCK.

Nyaberi, M. D., & Rop, B. K. (2014). Petroleum Prospects of Lamu Basin, South-Eastern Kenya. *Journal of the Geological Society of India, 83,* 414-422. https://doi.org/10.1007/s12594-014-0058-6

Nyagah, K. (1995). Stratigraphy, Depositional History and Environments of Deposition of Cretaceous through Tertiary Strata in the Lamu Basin, Southeast Kenya and Implications for Reservoirs for Hydrocarbon Exploration. *Sedimentary Geology, 96,* 43-71. https://doi.org/10.1016/0037-0738(94)00126-F

Nyagah, K., Cloeter, J., & Maende, A. (1996). Hydrocarbon Potential of the Lamu Basin of South-East Kenya. *AAPG Bulletin, 5*, Article No. CONF 960527.

Ombati, D., Githiri, J., K'Orowe, M., & Nyakundi, E. (2022). Delineation of Subsurface Structures Using Gravity Data of the Shallow Offshore, Lamu Basin, Kenya. *International Journal of Geophysics, 2022,* Article ID: 3024977. https://doi.org/10.1155/2022/3024977

Osicki, O., Schenk, O., & Kornpihl, D. (2015). *Prospectivity and Petroleum Systems Modeling of the Offshore Lamu Basin, Kenya: Implications for an Emerging Hydrocarbon Province*.

Osukuku, G., Osinowo, O., Sonibare, W., Makhanu, E., Rono, S., & Omar, A. (2022). Assessment of Hydrocarbon Generation Potential and Thermal Maturity of the Deep Offshore Lamu Basin, Kenya. *Energy Geoscience, 4,* 100133.

Pepper, A. S., & Corvi, P. J. (1995). Simple Kinetic Models of Petroleum Formation. Part I: Oil and Gas Generation from Kerogen. *Marine and Petroleum Geology, 12,* 291-319. https://doi.org/10.1016/0264-8172(95)98381-E

Peters, K. E., & Cassa, M. R. (1994). *Applied Source Rock Geochemistry: Chapter 5: Part II. Essential Elements*.

Ratnayake, A. S., Kularathne, C. W., & Sampei, Y. (2018). Assessment of Hydrocarbon Generation Potential and Thermal Maturity of the Offshore Mannar Basin, Sri Lanka. *Journal of Petroleum Exploration and Production Technology, 8,* 641-654. https://doi.org/10.1007/s13202-017-0408-1

Rop, B., & Patwardhan, A. (2013). The Hydrocarbon of Source Rocks Evaluation Study of Lokichar Basin, Northwestern Kenya. *Journal of the Geological Society of India, 81,* 575-580. https://doi.org/10.1007/s12594-013-0073-z

Ruffo, P., Bazzana, L., Consonni, A., Corradi, A., Saltelli, A., & Tarantola, S. (2006). Hydrocarbon Exploration Risk Evaluation through Uncertainty and Sensitivity Analysis Techniques. *Reliability Engineering & System Safety, 91,* 1155-1162. https://doi.org/10.1016/j.ress.2005.11.056

Steiner, S., Ahsan, S. A., Raina, I., Dasgupta, S., & Lis, G. P. (2016). Interpreting Total Organic Carbon TOC in Source Rock Oil Plays. In *The Abu Dhabi International Petroleum Exhibition & Conference*. https://doi.org/10.2118/183050-MS

Tissot, B. P., & Welte, D. H. (1984). Kerogen: Composition and Classification. In B. P. Tissot, & D. H. Welte (Eds.), *Petroleum Formation and Occurrence* (pp. 131-159). Springer. https://doi.org/10.1007/978-3-642-87813-8_9

Wang, X., Xie, R., Wang, T., Liu, R., & Shao, L. (2021). Total Organic Carbon Content Prediction of Source Rocks with Conventional Well Log Data Based on Regression Committee Machine. *Arabian Journal of Geosciences, 14,* Article No. 1. https://doi.org/10.1007/s12517-020-06304-8

Waples, D. W. (1994). *Maturity Modeling: Thermal Indicators, Hydrocarbon Generation, and Oil Cracking: Chapter 17: Part IV. Identification and Characterization*.

Zhou, Z. Y., Tao, Y., Li, S. J., & Ding, W. L. (2013). Hydrocarbon Potential in the Key Basins on the East Coast of Africa. *Petroleum Exploration and Development, 40,* 582-591. https://doi.org/10.1016/S1876-3804(13)60076-2

Appendix

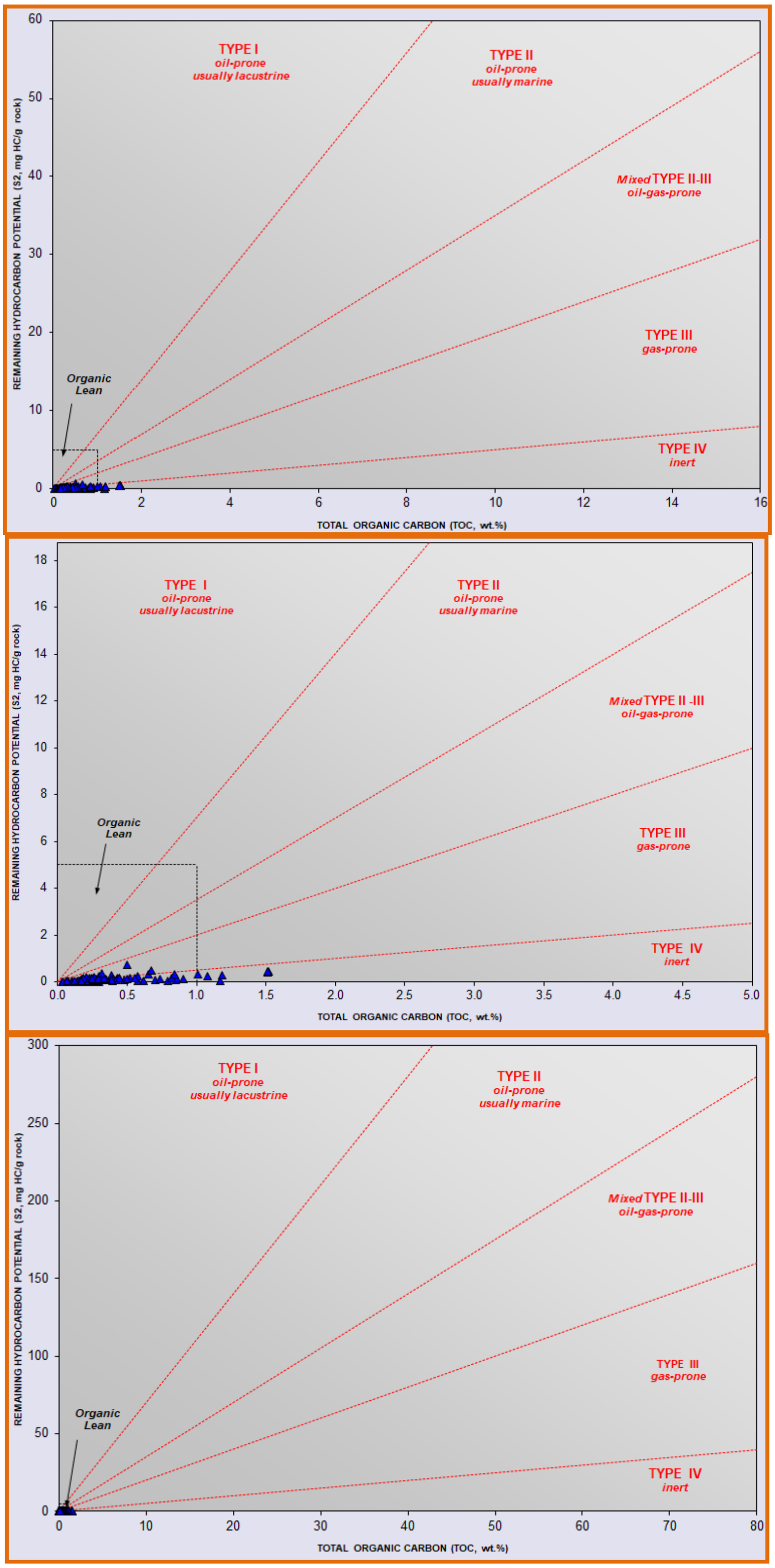

Figure A1. Kerogen quality plot for Mbawa-1 (modified from Weatherford laboratories).